Modeling IEEE 802.15.4 Networks Over Fading Channels

Piergiuseppe Di Marco, *Member, IEEE*, Carlo Fischione, *Member, IEEE*, Fortunato Santucci, *Senior Member, IEEE*, and Karl Henrik Johansson, *Fellow, IEEE*

***Abstract*—Although the performance of the medium access control (MAC) of the IEEE 802.15.4 has been investigated under the assumption of ideal wireless channel, the understanding of the cross-layer dynamics between MAC and physical layer is an open problem when the wireless channel exhibits path loss, multi-path fading, and shadowing. The analysis of MAC and wireless channel interaction is essential for consistent performance prediction, correct design and optimization of the protocols. In this paper, a novel approach to analytical modeling of these interactions is proposed. The analysis considers simultaneously a composite channel fading, interference generated by multiple terminals, the effects induced by hidden terminals, and the MAC reduced carrier sensing capabilities. Depending on the MAC parameters and physical layer thresholds, it is shown that the MAC performance indicators over fading channels can be far from those derived under ideal channel assumptions. As novel results, we show to what extent the presence of fading may be beneficial for the overall network performance by reducing the multiple access interference, and how this information can be used for joint selection of MAC and physical layer parameters.**

***Index Terms*—Fading channel, IEEE 802.15.4, interference, medium access control, multi-hop, WSN.**

I. Introduction

THE development of wireless sensor network (WSN) systems relies heavily on understanding the behavior of underlying communication mechanisms. When sensors and actuators are integrated within the physical world with large-scale and dense deployments, potential mobility of nodes, obstructions to propagation, fading of the wireless channel and multi-hop networking must be carefully addressed to offer reliable services. In fact, wireless interfaces can represent bottlenecks as they may not provide links as solid as required by applications in terms of reliability, delay, and energy.

Manuscript received July 16, 2013; revised November 25, 2013, March 13, 2014, and May 31, 2014; accepted July 30, 2014. Date of publication August 15, 2014; date of current version October 8, 2014. This work was supported in part by the Swedish Foundation for Strategic Research, the Swedish Research Council and the Knut and Alice Wallenberg Foundation, the EU projects Hydrobionets and Hycon2, and the PRIN Greta project (2010WHY5PR). Part of this work appears in the proceedings of the IEEE International Conference on Communications 2013. The associate editor coordinating the review of this paper and approving it for publication was S. Bahk.

P. Di Marco, C. Fischione, and K. H. Johansson are with the ACCESS Linnaeus Center, School of Electrical Engineering, Royal Institute of Technology, SE-100 44 Stockholm, Sweden (e-mail: pidm@kth.se; carlofi@kth.se; kallej@kth.se).

F. Santucci is with the Centre of Excellence DEWS, Department of Information Engineering, Computer Science and Mathematics (DISIM), University of L'Aquila, 67100 L'Aquila, Italy (e-mail: fortunato.santucci@univaq.it).

Color versions of one or more of the figures in this paper are available online at http://ieeexplore.ieee.org.

Digital Object Identifier 10.1109/TWC.2014.2349499

There is consensus that the protocols for physical layer and medium access control (MAC) for low data rate and low power applications in the future will be based on the flexible IEEE 802.15.4 standard with its numerous variants [1]. That standard has been indeed adopted with some modifications also by a number of other protocol stacks, including ZigBee, WirelessHART, ISA-100 [2]. It is already being used for applications in industrial control, home automation, health care, and smart grids. Nevertheless, as we discuss in the following, there is not yet a clear understanding of the cross layer interactions of the IEEE 802.15.4 protocol stack, with the consequent inability to adapt the communication performance (e.g., through cross-layer optimization) to meet challenging quality of service requirements.

The IEEE 802.15.4 MAC layer has received much attention, with focus on performance characterization in terms of reliability (i.e., successful packet reception probability), packet delay, throughput, and energy consumption. Some initial works, such as [3], are based on Monte Carlo simulations. More recent investigations have attempted to model the protocol performance by theoretical analysis for single hop networks [4]–[10]. These analytical studies are based on extensions of the Markov chain model originally proposed by Bianchi for the IEEE 802.11 MAC protocol [11] and assume ideal channel conditions.

The main limitation of the existing studies in literature is that MAC and physical layers analysis are investigated independently. In [12], modeling of packet losses due to channel fading have been introduced into the homogeneous Markov chain developed for the IEEE 802.15.4 MAC setup presented in [6]. However, fading is considered only for single packet transmission attempts, the effect of contention and multiple access interference is neglected, and the analysis is neither validated by simulations nor by experiments. In [13] the optimal carrier sensing range is derived to maximize the throughput for IEEE 802.11 networks; however, statistical modeling of wireless fading has not been considered, but a two-ray ground radio propagation model is used. Recent studies have investigated the performance of multiple access networks in terms of multiple access interference and capture effect for IEEE 802.11 MAC in [14]–[17] and for IEEE 802.15.4 MAC in [18]. However, the models in [14]–[16], [18] are limited to homogeneous networks (same statistical model for every node) with homogeneous traffic and uniform random deployment. Heterogeneous traffic conditions are discussed in [17], by assuming two classes of traffics. It is worthwhile mentioning that the models in [16], [17] represent the state of the art for the analysis of the IEEE 802.11 MAC over fading channels. Nevertheless, they consider

only multi-path fading and the statistics are derived under the assumption of perfect power control and perfect carrier sensing. The model in [18] assumes that nodes are synchronized and a single packet transmission for each node is considered. Thus, the number of contending nodes in transmission is known at the beginning of the superframe. We consider instead a setup with asynchronous Poisson traffic generation, which is more general. Moreover, in [18] the channel is characterized on a distance-based model, and the effect of aggregated shadowing and multi-path components has not been considered, while it is known that it has a crucial impact on the performance of packet access mechanisms [19].

In all the aforementioned studies, the probability of fading and capture are evaluated in terms of average effects of the network on the tagged node. There is actually a closer interaction between MAC and physical channel. For instance, a bad channel condition during the channel sensing procedure can be interpreted as an idle channel condition for the tagged node, therefore causing potential collisions. However, a bad channel condition for the contenders can imply a higher probability of success for the tagged node. These situations cannot be modeled by using existing analytical studies for homogeneous IEEE 802.15.4 networks (e.g., [18]). Similarly, the interactions between MAC and physical channel cannot be predicted by existing models for heterogeneous IEEE 802.15.4 networks (e.g., [20]), since only ideal channel conditions are considered. Finally, we remark that the combined effects of fading and multiple access interference cannot be distinguished just by mean of experimental evaluations [18].

In this paper we propose a novel analytical model that captures the cross-layer interactions of IEEE 802.15.4 MAC and physical layer over interference-limited wireless channels with composite fading models. The main original contributions are as follows.

- We propose a general modeling approach for characterization of the MAC performance with heterogeneous network conditions, a composite Nakagami-lognormal channel, explicit interference behaviors and cross-layer interactions.
- Based on the new model, we determine the impact of fading conditions on the MAC performance under various settings for traffic, inter-node distances, carrier sensing range, and signal-to-(interference plus noise)-ratio (SINR). We show how existing models of the MAC from the literature may give unsatisfactory or inadequate predictions for performance indicators in fading channels.
- We discuss system configurations in which a certain severity of the fading may be beneficial for overall network performance. Based on the new model, it is then possible to derive optimization guidelines for the overall network performance, by leveraging on the MAC-physical layer interactions.

To determine the network operating point and the performance indicators in terms of reliability, delay, and energy consumption for single-hop and multi-hop topologies, a moment matching approximation for the linear combination of lognormal random variables based on [21] and [22] is adopted to build a Markov chain model of the MAC mechanism that embeds the physical layer behavior. The challenging part of the new analytical setup proposed in this paper is to model the complex interaction between the MAC protocol and the wireless channel with explicit description of the dependence on several topological parameters and network dynamics. For example, we include failures of the channel sensing mechanism and the presence of hidden terminals, namely nodes that are in the communication range of the destination but cannot be heard by the transmitter. Whether two wireless nodes can communicate with each other depends on their relative distance, the transmission power, the wireless propagation characteristics and interference caused by concurrent transmissions on the same radio channel: the higher the SINR is, the higher the probability that packets can be successfully received. The number of concurrent transmissions depends on the traffic and the MAC parameters. To the best of our knowledge, this is the first paper that accounts for statistical fluctuations of the SINR in the Markov chain model of the IEEE 802.15.4 MAC.

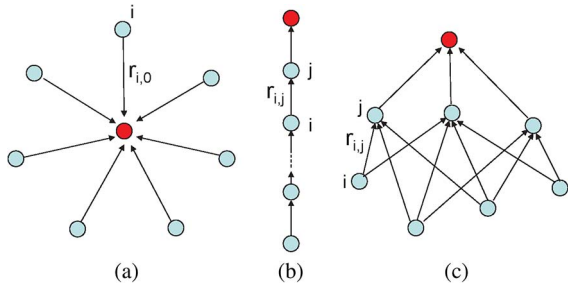

Fig. 1. Example of topologies: (a) single-hop star topology, (b) multi-hop linear topology, and (c) multi-hop topology with multiple end-devices.

The remainder of the paper is organized as follows. In Section II, we introduce the network model. In Section III, we derive an analytical model of IEEE 802.15.4 MAC over fading channels. In Section IV, reliability, delay, and energy consumption are derived. The accuracy of the model is evaluated in Section V, along with a detailed analysis of performance indexes with various parameter settings. Section VI concludes the paper and prospects our future work.

II. Network Model

We illustrate the network model by considering the three topologies sketched in Fig. 1. Nevertheless, the analytical results that we derive in this paper are applicable to any fixed topology.

The topology in Fig. 1(a) refers to a single-hop (star) network, where node i is deployed at distance $r_{i,0}$ from the root node at the center, and where nodes forward their packets with single-hop communication to the root node. The topology in Fig. 1(b) is a multi-hop linear topology, where every node generates and forwards traffic to the root node by multi-hop communication. The distance between two adjacent nodes is denoted as $r_{i,j}$. In Fig. 1(c), we illustrate a multi-hop topology with multiple end-devices that generate and forward traffic according to an uplink routing policy to the root node.

Consider node i that is transmitting a packet with transmission power $P_{\mathrm{tx},i}$. We consider an inverse power model of the link gain, and include shadowing and multi-path fading as well.

The received power at node j, which is located at a distance $r_{i,j}$, is then expressed as follows

$$P_{\mathrm{rx},i,j} = \frac{c_0 P_{\mathrm{tx},i}}{r_{i,j}^k} f_i \exp(y_i). \quad (1)$$

The constant c_0 represents the power gain at the reference distance 1 m, and it can account for specific propagation environments and parameters, e.g., carrier frequency and antennas. In the operating conditions for IEEE 802.15.4 networks, the inverse of c_0 (i.e., the path loss at the reference distance) is in the range 40–60 dB [1]. The exponent k is called path loss exponent, and varies according to the propagation environment in the range 2–4. The factor f_i models a frequency-flat channel fading due to multi-path propagation, which we assume to follow a Nakagami distribution with parameter $\kappa \geq 0.5$ and p.d.f.

$$p_{f_i}(z) = \kappa^\kappa \frac{(z)^{\kappa-1}}{\Gamma(\kappa)} \exp(-\kappa z),$$

where $\Gamma(\kappa)$ is the standard Gamma function $\Gamma(\kappa) = \int_0^\infty \exp(-x) x^{\kappa-1} dx$. We consider the Nakagami distribution since it is a general statistical model and it captures fading environments with various degrees of severity, including Rayleigh and Rice environments. A lognormal random component models the shadowing effects due to obstacles, with $y_i \sim \mathcal{N}(0, \sigma_i^2)$. The standard deviation σ_i is called spread factor of the shadowing. These assumptions are accurate for IEEE 802.15.4 in a home or urban environment where devices may not be in visibility.

In the rest of the paper, we use the index l as a short form to denote a link between the transmitting node i and the receiving node j. We use the double indices (i, j) for variables that depend on a generic pair of nodes in the network. In the following section, a generalized model of a heterogeneous network using unslotted IEEE 802.15.4 MAC over multi-path fading channels is proposed.

III. IEEE 802.15.4 MAC AND PHY LAYER MODEL

In this section we propose a novel analytical setup to derive the network performance indicators, namely the reliability as probability of successful packet reception, the delay for successfully received packets, and the average node energy consumption. We first consider a single-hop case, and then we generalize the model to the multi-hop case.

A. Unslotted IEEE 802.15.4 MAC Mechanism

According to the IEEE 802.15.4 MAC, each link can be in one of the following states: (i) idle state, when the transmitting node is waiting for the next packet to be generated; (ii) backoff state; (iii) clear channel assessment (CCA) state; (iv) transmission state.

Let the link l be in idle state. Three variables given by the number of backoffs NB, backoff exponent BE, and retransmission attempts RT are initialized: the default initialization is $NB := 0$, $BE := macMinBE$, and $RT := 0$. Note that we use the italic for the MAC variables, as these are the conventional names used in the standard [1]. From idle state, a transmitting node wakes up with probability q_l, which represents the packet generation probability in each time unit of duration $aUnitBackoffPeriod$, and moves to the first backoff state, where the node waits for a random number of complete backoff periods in the range $[0, 2^{BE} - 1]$ time units.

When the backoff period counter reaches zero, the node performs the CCA procedure. If the CCA fails due to busy channel, the value of both NB and BE is increased by one. Once BE reaches its maximum value $macMaxBE$, it remains at the same value until it is reset. If NB exceeds its threshold $macMaxCSMABackoffs$, the packet is discarded due to channel access failure. Otherwise the MAC algorithm generates again a random number of complete backoff periods and repeats the procedure. If the CCA is successful, the packet is transmitted. The reception of the corresponding ACK is interpreted as successful packet transmission. Otherwise, the variable RT is increased by one, the MAC layer initializes $BE := macMinBE$ and starts again the MAC mechanism to re-access the channel. If RT is greater than its threshold $macMaxFrameRetries$, the packet is discarded as the retry limit is exceeded.

In the following, we indicate the probability of being in CCA state by τ_l, the probability that the channel is sensed busy as busy channel probability, denoted by α_l, and the probability of unsuccessful packet transmission as packet loss probability, denoted by γ_l. Moreover, we denote the MAC parameters by $m_0 \triangleq macMinBE$, $m_b \triangleq macMaxBE$, $m \triangleq macMaxCSMABackoffs$, $n_r \triangleq macMaxFrameRetries$, and $S_b \triangleq aUnitBackoffPeriod$. A list of the main symbols used in the paper is reported in Appendix C.

B. MAC-Physical Layer Model

In this subsection, the MAC model presented in [20], which was developed for ideal channel conditions, is substantially modified and extended to include the main features of real channel impairments and interference.

Let us assume that packets are generated by node i according to the Poisson distribution with rate λ_i. The probability of generation of a new packet after an idle unit time is then $q_l = 1 - \exp(-\lambda_i / S_b)$. Notice that the index l refers to the link l, but the expression of q_l depends only on the index i of the transmitting node. For a single-hop network, the parameters related to link l can be uniquely associated to the index i of the transmitting node. This is not true in general for multi-hop networks, where more than one link can be associated to the same transmitting node, as we discuss later in Section III-D.

Queueing effects and a limited buffer size B are considered in the MAC model under the assumption that the node buffer is modeled as a $M/G/1/K$ queueing system. The probabilities that the node queue is not empty i) after a packet has been successfully sent $q_{\mathrm{succ},l}$, ii) after a packet has been discarded due to channel access failure $q_{\mathrm{cf},l}$ or iii) due to the retry limit $q_{\mathrm{cr},l}$ are derived in Appendix A.

We define the packet successful transmission time L_s and the packet collision time L_c as

$$\begin{aligned} L_s &= L + t_{\text{ack}} + L_{\text{ack}} + IFS, \\ L_c &= L + t_{\text{m,ack}}, \end{aligned} \tag{2}$$

where L is the total length of a packet including overhead and payload, t_{ack} is ACK waiting time, L_{ack} is the length of ACK frame, IFS is the inter-frame spacing, and $t_{\text{m,ack}}$ is the timeout (waiting for the ACK) in the retransmission algorithm, as detailed in [1].

The time unit for all parameters and variables is S_b, which corresponds to the transmission time of 20 symbols [1]. When performing the CCA, a node is listening in RX mode for a duration of 8 symbols. Then the nodes takes a time of 12 symbols ($aTurnaroundTime$) to turn around from RX mode to TX mode before starting the transmission of the packet, which makes a total time of 20 symbols (S_b) for a successful CCA. Therefore, it is possible to conclude that S_b is accurate enough to capture the main characteristics of the MAC mechanism for a transmitting node.

By using Proposition 4.1 in [20], the CCA probability τ_l can be expressed as a function of the packet generation probability q_l, the busy channel probability α_l, the packet loss probability γ_l, and the MAC parameters m_0, m_b, m, and n_r as

$$\tau_l = \left(\frac{1-\alpha_l^{m+1}}{1-\alpha_l}\right)\left(\frac{1-\xi_l^{n_r+1}}{1-\xi_l}\right) b_{0,0,0}^{(l)}, \tag{3}$$

where

$$b_{0,0,0}^{(l)} = \begin{cases} \left[\frac{1}{2}\left(\frac{1-(2\alpha_l)^{m+1}}{1-2\alpha_l}2^{m_0} + \frac{1-\alpha_l^{m+1}}{1-\alpha_l}\right)\frac{1-\xi_l^{n_r+1}}{1-\xi_l} \right. \\ \quad + (L_s(1-\gamma_l)+L_c\gamma_l)(1-\alpha^{m+1})\frac{1-\xi_l^{n_r+1}}{1-\xi_l} \\ \quad + \frac{1-q_{cf,l}}{q_l}\frac{\alpha_l^{m+1}\left(1-\xi_l^{n_r+1}\right)}{1-\xi_l} + \frac{1-q_{cr,l}}{q_l}\xi_l^{n_r+1} \\ \quad \left. + \frac{1-q_{\text{succ},l}}{q_l}(1-\gamma_l)\frac{\left(1-\alpha_l^{m+1}\right)\left(1-\xi_l^{n_r+1}\right)}{1-\xi_l}\right]^{-1}, \\ \qquad\qquad \text{if } m \le \bar{m} = m_b - m_0, \\ \left[\frac{1}{2}\left(\frac{1-(2\alpha_l)^{\bar{m}+1}}{1-2\alpha_l}2^{m_0} + \frac{1-\alpha_l^{\bar{m}+1}}{1-\alpha_l}\right.\right. \\ \quad \left.\left. + (2^{m_b}+1)\alpha_l^{\bar{m}+1}\frac{1-\alpha_l^{m-\bar{m}}}{1-\alpha_l}\right)\frac{1-\xi_l^{n_r+1}}{1-\xi_l}\right. \\ \quad + (L_s(1-\gamma_l)+L_c\gamma_l)(1-\alpha_l^{m+1})\frac{1-\xi_l^{n_r+1}}{1-\xi_l} \\ \quad + \frac{1-q_{cf,l}}{q_l}\frac{\alpha_l^{m+1}(1-\xi_l^{n_r+1})}{1-\xi_l} + \frac{1-q_{cr,l}}{q_l}\xi_l^{n_r+1} \\ \quad \left. + \frac{1-q_{\text{succ},l}}{q_l}(1-\gamma_l)\frac{(1-\alpha_l^{m+1})(1-\xi_l^{n_r+1})}{1-\xi_l}\right]^{-1}, \\ \qquad\qquad \text{otherwise}, \end{cases} \tag{4}$$

and $\xi_l = \gamma_l(1-\alpha_l^{m+1})$. Details on the derivation of Eqs. (3) and (4) are reported in Appendix B.

The expression of the CCA probability in Eq. (3) abstracts the behavior of the MAC independently of the underlying physical layer and channel conditions, which we include in the following by deriving novel expressions of the busy channel probability α_l and packet loss probability γ_l.

The busy channel probability can be decomposed as

$$\alpha_l = \alpha_{\text{pkt},l} + \alpha_{\text{ack},l}, \tag{5}$$

where $\alpha_{\text{pkt},l}$ is the probability that node i senses the channel and finds it occupied by an ongoing packet transmission, whereas $\alpha_{\text{ack},l}$ is the probability of finding the channel busy due to ACK transmission. Next we derive these probabilities.

The busy channel probability due to packet transmissions evaluated at node i is the combination of three events: i) at least one other node has accessed the channel within one of the previous L units of time; ii) at least one of the nodes that had accessed the channel found it idle and started a transmission; iii) the total received power at node i is larger than a threshold a, so that an ongoing transmission is detected by node i.

The combination of all busy channel events yields the busy channel probability that the transmitting node i in link l senses the channel and finds it occupied by an ongoing packet transmission

$$\alpha_{\text{pkt},l} = L\mathcal{H}_l\left(\mathbf{p}_i^{\text{det}}\right), \tag{6}$$

where

$$\begin{aligned} \mathcal{H}_l(\boldsymbol{\chi}) = \sum_{v=1}^{N-1}\sum_{j=1}^{C_{N-1,v}} \Bigg(& \prod_{k=1}^{v}\tau_{k_j}\prod_{h=v+1}^{N-1}(1-\tau_{h_j}) \\ & \times \sum_{x=1}^{v}\sum_{n=1}^{C_{v,x}}\left(\prod_{z=1}^{x}(1-\alpha_{z_n})\chi(x,n)\prod_{r=x+1}^{v}\alpha_{r_n}\right)\Bigg) \end{aligned} \tag{7}$$

represents the probability of concurrent transmissions starting in a given time unit, as a function of the elements of the matrix $\boldsymbol{\chi}$. The first double sum in v and j enumerates the $C_{N-1,v} = \binom{N-1}{v}$ combinations of events in which v nodes access the channel in a given time unit (excluding the transmitting node i). The second double sum in x and n considers the events of x successful CCAs. Given N nodes in the network, the subscript k_j refers to the node in the k-th position in the j-th combination of v out of $N-1$ elements. The actual node index depends on the ordering of elements in the combination: e.g., if we select nodes $\{1, 2, \ldots, v\}$ for $j = 1$, we select $\{1, 3, \ldots, v+1\}$ for $j = 2$, and so on, when expanding τ_{k_j}, we have $\tau_{1_1} = \tau_1$, $\tau_{1_2} = \tau_2$, $\tau_{2_1} = \tau_2$, $\tau_{2_2} = \tau_3$, and so on. The subscript z_n refers to the node in the z-th position in the n-th combination of x out of v elements. For all the combinations of x simultaneous transmissions, the busy channel probability $\alpha_{\text{pkt},l}$ is evaluated as a function of the detection probabilities at the transmitting node i.

We consider a matrix $\mathbf{p}_i^{\text{det}}$ of dimension $(N-1)\times 2^{(N-1)}$, whose element $p_i^{\text{det}}(x,n)$ is the probability that the received power by the n-th combination of x contending nodes to node i is larger than a threshold a, i.e.,

$$p_i^{\text{det}}(x,n) = \Pr\left[\sum_{z=1}^{x} P_{\text{rx},z_n,i} > a\right]. \tag{8}$$

Notice that Eq. (6) is obtained under static (fully correlated) channel conditions within a packet transmission time. In other

words, we assume that the average energy level captured in a time unit S_b is representative of the average energy level during any of L consecutive time units. The assumption is consistent with the IEEE 802.15.4 MAC protocol.

The busy channel probability due to an ACK transmission, recall Eq. (5), follows from a similar derivation. An ACK is sent only after a successful packet transmission. Therefore,

$$\alpha_{\mathrm{ack},l} = L_{\mathrm{ack}} \mathcal{H}_l \left(\bar{\mathbf{p}}_i^{\mathrm{det}} \right),$$

where $\bar{\mathbf{p}}_i^{\mathrm{det}}$ is a matrix of dimension $(N-1) \times 2^{(N-1)}$ with $\bar{p}_i^{\mathrm{det}}(x,n) = (1-\gamma_{z_n}) p_i^{\mathrm{det}}(x,n)$, and L_{ack} is the length of the ACK.

We next derive an expression for the packet loss probability γ_l, namely the probability that a transmitted packet from node i is not correctly received by node j. A packet transmission is not correctly received if there is at least one interfering node whose transmission partially (or fully) overlaps and the SINR between the received power from the intended transmitter and the total interfering power plus the noise power level N_0 is lower than a threshold b (outage). In the event of no active interferers, which occurs with probability $1 - \mathcal{H}_l(\mathbf{1})$[1], the packet loss probability is the probability that the signal-to-noise ratio (SNR) between the received power and the noise level is lower than b. Hence

$$\gamma_l = (1 - \mathcal{H}_l(\mathbf{1}))\, p_{i,j}^{\mathrm{fad}} + \mathcal{H}_l \left(\mathbf{p}_{i,j}^{\mathrm{out}} \right) + (2L-1) \mathcal{H}_l \left(\left(1 - \mathbf{p}_i^{\mathrm{det}}\right) \star \mathbf{p}_{i,j}^{\mathrm{out}} \right), \quad (9)$$

where $\mathbf{p}_{i,j}^{\mathrm{out}}$ is the matrix of outage probabilities in the presence of interferers (with composite and different channel fading on every link),

$$p_{i,j}^{\mathrm{out}}(x,n) = \Pr\left[\frac{P_{\mathrm{rx},i,j}}{\sum_{z=1}^{x} P_{\mathrm{rx},z_n,j} + N_0} < b \right], \quad (10)$$

and $p_{i,j}^{\mathrm{fad}}$ is the outage probability due to composite channel fading on the useful link (i,j) with no interferers,

$$p_{i,j}^{\mathrm{fad}} = \Pr\left[\frac{P_{\mathrm{rx},i,j}}{N_0} < b \right]. \quad (11)$$

Note that the symbol $\star$ represents the Hadamard product.

The expressions of the carrier sensing probability τ_l in Eq. (3), the busy channel probability α_l in Eq. (5), the collision probability in Eq. (9), for $l = 1, \ldots, N$, form a system of non-linear equations that can be solved through numerical methods [23].

We next need to derive the detection probability and the outage probabilities in the devised wireless context. With such a goal in mind, we present some useful intermediate results in the following section.

C. Model of Aggregate Multi-Path Shadowed Signals

In this section, we consider the problem of computing the sum of multi-path shadowed signals that appear in the detection probability and in the outage probability. The analysis follows the approach developed in [21] and [22] for cellular systems, adapting the model to the characteristics of random access systems.

Consider the transmitting node i performing a CCA and let us focus our attention on the detection probability in transmission in Eq. (8). Without loss of generality, in the rest of the section we replace the double index z_n with z, keeping it associated to the the node in the z-th position in the n-th combination of x out of v elements, as explained in the previous section. Therefore, we consider $\Pr[\sum_{z=1}^{x} P_{\mathrm{rx},z,i} > a]$, where x is the current number of active nodes in transmission. By recalling the power channel model in Eq. (1), let us define the random variable $Y_i = \ln(\sum_{z=1}^{x} A_{i,z} \exp(y_z))$, with $A_{i,z} = c_0 P_{\mathrm{tx},z} f_z / r_{z,i}^k$, and $y_z \sim \mathcal{N}(0, \sigma_z^2)$. Since a closed form expression of the probability distribution function of Y_i does not exist, we resort to a useful approximation instead. To characterize Y_i, we apply the Moment Matching Approximation (MMA) method, which approximates the statistics of linear combination of lognormal components with a lognormal random variable, such that $Y_i \sim \mathcal{N}(\eta_{Y_i}, \sigma_{Y_i}^2)$. According to the MMA method, η_{Y_i} and σ_{Y_i} can be obtained by matching the first two moments of $\exp(Y_i)$ with the first two moments of $\sum_{z=1}^{x} A_{i,z} \exp(y_z)$, i.e.,

$$M_1 \triangleq \exp\left(-\eta_{Y_i} + \frac{\sigma_{Y_i}}{2} \right) = \sum_{z=1}^{x} E\{A_{i,z}\} \exp\left(\frac{\sigma_{y_z}}{2} \right), \quad (12)$$

$$M_2 \triangleq \exp\left(-2\eta_{Y_i} + 2\sigma_{Y_i}\right) = \sum_{u=1}^{x} \sum_{z=1}^{x} E\{A_{i,u} A_{i,z}\} \exp\left(\frac{\sigma_{y_u}^2 + \sigma_{y_z}^2}{2} + \rho_{y_u, y_z} \sigma_{y_u} \sigma_{y_z} \right). \quad (13)$$

Solving Eqs. (12), and (13) for η_{Y_i} and σ_{Y_i} yields $\eta_{Y_i} = 0.5 \ln(M_2) - 2\ln(M_1)$, and $\sigma_{Y_i}^2 = \ln(M_2) - 2\ln(M_1)$.

It follows that

$$p_i^{\mathrm{det}} = \Pr\left[\exp(Y_i) > a\right] \approx Q\left(\frac{\ln(a) - \eta_{Y_i}}{\sigma_{Y_i}} \right), \quad (14)$$

where $Q(\xi) = (1/\sqrt{2\pi}) \int_{\xi}^{\infty} \exp(-(\nu^2/2))\, d\nu$. To simplify the notation, we denote by p_i^{det} the element $p_i^{\mathrm{det}}(x,n)$ of $\mathbf{p}_i^{\mathrm{det}}$.

Similar derivations follow for the outage probability in reception

$$\Pr\left[\frac{P_{\mathrm{rx},i,j}}{\sum_{z=1}^{x} P_{\mathrm{rx},z,j} + N_0} < b \right] = \Pr\left[f_i \left(\sum_{z=1}^{x} \frac{P_{\mathrm{tx},z} r_{i,j}^k}{P_{\mathrm{tx},i} r_{z,j}^k} \frac{f_z \exp(y_z)}{\exp(y_i)} + \frac{N_0 r_{i,j}^k}{P_{\mathrm{tx},i}} \frac{f_z}{\exp(y_i)} \right)^{-1} < b \right].$$

Let us now define the random variable $\tilde{Y}_{i,j} = -\ln(\sum_{z=1}^{x+1} B_{i,j,z} \exp(\tilde{y}_z))$, where $B_{i,j,z} = (P_{\mathrm{tx},z} r_{i,j}^k / P_{\mathrm{tx},i} r_{z,j}^k) f_z$ for $z = 1, \ldots, x$, $B_{i,j,z} = (N_0 r_{i,j}^k / P_{\mathrm{tx},i}) f_z$ for $z = x+1$, $\tilde{y} = y_z - y_i$ for $z = 1, \ldots, x$, and $\tilde{y} = -y_i$ for $z = x+1$.

According to the MMA method, we approximate $\tilde{Y}_i \sim \mathcal{N}(\eta_{Y_i}, \sigma_{Y_i}^2)$, where $\eta_{\tilde{Y}_{i,j}}$ and $\sigma_{\tilde{Y}_{i,j}}$ can be obtained by matching

[1] We define $\mathbf{1}$ as a matrix of dimension $(N-1) \times 2^{(N-1)}$ with all ones.

the first two moments of $\exp(\tilde{Y}_i)$ with the first two moments of $\sum_{z=1}^{N} B_{i,j,z}\exp(\tilde{y}_z)$, i.e.,

$$\tilde{M}_1 \triangleq \exp\left(-\eta_{\tilde{Y}_{i,j}}+\frac{1}{2}\sigma_{\tilde{Y}_{i,j}}\right)=\sum_{z=1}^{x+1}E\{B_{i,j,z}\}\exp\left(\frac{\sigma_{\tilde{y}_z}}{2}\right),$$

$$\tilde{M}_2 \triangleq \exp\left(-2\eta_{\tilde{Y}_{i,j}}+2\sigma_{\tilde{Y}_{i,j}}\right)$$
$$=\sum_{u=1}^{x+1}\sum_{z=1}^{x+1}E\{B_{i,j,u}B_{i,j,z}\}\exp\left(\frac{\sigma^2_{\tilde{y}_u}}{2}+\frac{\sigma^2_{\tilde{y}_z}}{2}+\rho_{\tilde{y}_u,\tilde{y}_z}\sigma_{\tilde{y}_u}\sigma_{\tilde{y}_z}\right),$$

$\eta_{\tilde{Y}_{i,j}} = 0.5\ln(\tilde{M}_2) - 2\ln(\tilde{M}_1)$, $\sigma^2_{\tilde{Y}_{i,j}} = \ln(\tilde{M}_2) - 2\ln(\tilde{M}_1)$. Therefore, we obtain

$$p^{\text{out}}_{i,j} = \Pr\left[f_i\exp(\tilde{Y}_{i,j}) < b\right]$$
$$=\int_0^b\int_0^\infty p_f(q|w)\frac{1}{\sqrt{2\pi}\sigma_{\tilde{Y}_{i,j}}w}\exp\left(-\frac{(\ln(w)-\eta_{\tilde{Y}_i})^2}{2\sigma^2_{\tilde{Y}_i}}\right)dw\,dq. \tag{15}$$

By considering the limit case with $x = 0$, we obtain the expression for the outage probability with no interferers presented in Eq. (11). By denoting $C_{i,j} = P_{\text{tx},i}/(r^k_{z,j}N_0)$, we have

$$p^{\text{fad}}_{i,j} = \Pr[C_{i,j}f_i\exp(y_i) < b]$$
$$=\int_0^b\int_0^\infty p_f(q|w)\frac{1}{\sqrt{2\pi}\sigma_i w}\exp\left(-\frac{(\ln(w)-\ln(C_{i,j}))^2}{2\sigma_i^2}\right)dw\,dq. \tag{16}$$

The analysis above holds for a generic weighted composition of lognormal fading components. In the case of lognormal channel model, where only shadow fading components are considered, (i.e., $f_i = 1$), the outage probability becomes

$$p^{\text{out,L}}_{i,j} = \Pr\left[\exp(\tilde{Y}_{i,j}) < b\right] \approx 1-Q\left(\frac{\ln(b)-\eta_{\tilde{Y}_{i,j}}}{\sigma_{\tilde{Y}_{i,j}}}\right). \tag{17}$$

For a Nakagami-lognormal channel,

$$p^{\text{out,NL}}_{i,j} = \int_0^\infty \frac{1}{\sqrt{2\pi}\sigma_{\tilde{Y}_{i,j}}w}\exp\left(-\frac{(\ln(w)-\eta_{\tilde{Y}_i})^2}{2\sigma^2_{\tilde{Y}_i}}\right)$$
$$\times\int_0^b \kappa^\kappa\frac{(qw)^{\kappa-1}}{\Gamma(\kappa)}\exp(-\kappa qw)\,dq\,dw.$$

For integer values of κ, the integration in q yields

$$p^{\text{out,NL}}_{i,j} = 1-\int_0^\infty \frac{1}{\sqrt{2\pi}\sigma_{\tilde{Y}_{i,j}}w}\exp\left(-\frac{(\ln(w)-\eta_{\tilde{Y}_i})^2}{2\sigma^2_{\tilde{Y}_i}}\right)$$
$$\times\sum_{i=0}^{\kappa-1}\frac{(\kappa bw)^i}{\Gamma(i+1)}\exp(-\kappa bw)\,dw.$$

The mean and standard deviation of Y_i and $\tilde{Y}_{i,j}$ can be obtained by inserting the moments of f_i in the moments of $A_{i,z}$ and $B_{i,j,z}$. For Gamma distributed components f_i, we obtain $E\{f_i\} = 1$ and $E\{f_i^2\} = (\kappa+1)/\kappa$.

We remark here that the evaluation of p^{det}_i in Eq. (14), $p^{\text{out}}_{i,j}$ in Eq. (15), and $p^{\text{fad}}_{i,j}$ in Eq. (16) can be carried out off-line with respect to the solution of the system of nonlinear equations that need to be solved when deriving τ_l, α_l and γ_l, where these probabilities are used. Therefore, the proposed model can be implemented with only a slight increase of complexity with respect to the analytical model of the IEEE 802.15.4 MAC mechanism presented in [20], but the online computation time is not affected significantly.

D. Extended Model for Multi-Hop Networks

Here we extend the analytical model to a more general network in which information is collected through a multi-hop communication via static routing towards a sink node.

The model equations derived in Section III-B are solved for each link $l = 1,\ldots,G$ of the network, by considering that the probability q_l of having a packet to transmit in each time unit does not depend only on the generated traffic λ_i from the transmitting node i, but also on the traffic to forward from children nodes according to the routing policy. The effect of routing are described by the routing matrix $\mathbf{M}$, such that $M_{i,j} = 1$ if node j is selected as the forwarding node for the traffic of node i, and $M_{i,j} = 0$ otherwise. We assume that the routing matrix is built such that no cycles exists. In the case of multiple candidate parents (one-hop destinations) at node i, we define $M_{i,j} = \tilde{q}_{i,j}$ where $\tilde{q}_{i,j} < 1$ is the proportion of traffic from node i that is forwarded to node j. In the implementation of the protocol, a single queue per node is typically considered. Therefore, there is no possibility of simultaneous transmissions from the same transmitter node along different links, such as along link (i,j) and link (i,k). In the model, however, we consider independent channel access probabilities among different links, so that transmissions along link (i,j) and link (i,k) can be made simultaneously. As we show in Section V, this simplifying assumption does not affect the accuracy of the results.

We define the traffic distribution matrix $\mathbf{T}$ by scaling $\mathbf{M}$ by the probability of successful reception in each link as only successfully received packets are forwarded, i.e., $T_{i,j} = M_{i,j}R_l$, where the reliability R_l is derived next in Section IV-A. The vector of traffic generation probabilities Q is given in [20] by

$$Q = \lambda[\mathbf{I}-\mathbf{T}]^{-1}, \tag{18}$$

where $\mathbf{I} \in \mathbb{R}^{(N+1)\times(N+1)}$ is the identity matrix. The elements of Q affect also the other packet generation probabilities, i.e., $q_{\text{succ},l}$, $q_{\text{cf},l}$, and $q_{\text{cr},l}$ as described in Appendix A.

Equation (18) gives the relation between MAC and routing through the idle packet generation probability q_l. To include the effects of fading channels in the multi-hop network model, we couple Eq. (18) with the expressions for τ_l and α_l, as obtained by Eqs. (3), and (5). Moreover, to complete the model, we need

to derive the expression of the reliability R_l, as we illustrate in the following section.

IV. Performance Indicators

In this section, we investigate three major indicators to analyze the performance of the IEEE 802.15.4 MAC over fading channels. These indicators will also be used to validate the analytical model we derived in the previous section, by comparing results obtained from the (approximate) model with those obtained by extensive simulation campaigns. The first one is the reliability, evaluated as successful packet reception probability. Then we consider the delay for the successfully received packets as the time interval from the instant the packet is ready to be transmitted, until an ACK for such a packet is received. Eventually, we consider the energy consumption of network nodes.

A. Reliability

For each node of the network, the reliability is based on the probability that packets are discarded at MAC layer. In the unslotted IEEE 802.15.4 MAC, packets are discarded due to either (i) channel access failure or (ii) retry limits. A channel access failure happens when a packet fails to obtain clear channel within $m+1$ backoff stages in the current transmission attempt. Furthermore, a packet is discarded if the transmission fails due to repeated packet losses after n_r+1 attempts. According to the IEEE 802.15.4 MAC mechanism described in Section III-A, the probability that the packet is discarded due to channel access failure can be expressed as

$$p_{\mathrm{cf},l} = \alpha_l^{m+1} \sum_{j=0}^{n_r} \left(\gamma_l \left(1-\alpha_l^{m+1}\right)\right)^j,$$

and the probability of a packet being discarded due to retry limits is

$$p_{\mathrm{cr},l} = \left(\gamma_l \left(1-\alpha_l^{m+1}\right)\right)^{n_r+1}.$$

Therefore, the reliability $R_l = 1 - p_{\mathrm{cf},l} - p_{\mathrm{cr},l}$ is derived as

$$R_l = 1 - \alpha_l^{m+1} \frac{\left(1-\left(\gamma_l\left(1-\alpha_l^{m+1}\right)\right)^{n_r+1}\right)}{1-\gamma_l\left(1-\alpha_l^{m+1}\right)} - \left(\gamma_l\left(1-\alpha_l^{m+1}\right)\right)^{n_r+1}. \quad (19)$$

It is worthwhile mentioning that the last expressions embed the link between the reliability at the MAC level and the statistical description of wireless channel environment through Eq. (9) and the analysis of Section III-C. We do not include in the analysis the effects of buffer overflows on the reliability, as we assume that the maximum queue length at MAC layer is lower than the available buffer capacity, (see Appendix A).

B. Delay

We study the delay D_l for successfully delivered packets in the link l. If a packet is discarded due to either the limited number of backoff stages m or the finite retry limit n_r, its delay is not included in the computation.

Let $D_{l,h}$ be the delay for the transmitting node that sends a packet successfully at the h-th attempt. The expected value of the delay is

$$\mathbb{E}[D_l] = \sum_{h=0}^{n} \Pr[\mathscr{C}_h|\mathscr{C}]\,\mathbb{E}[D_{l,h}], \quad (20)$$

where the event $\mathscr{C}_h$ denotes the occurrence of a successful packet transmission at the attempt $h+1$ given h previous unsuccessful transmissions, whereas the event $\mathscr{C}$ indicates a successful packet transmission within n_r+1 attempts. Therefore, we can derive

$$\Pr[\mathscr{C}_h|\mathscr{C}] = \frac{\gamma_l^h\left(1-\alpha_l^{m+1}\right)^h}{\sum_{k=0}^{n_r}\left(\gamma_l\left(1-\alpha_l^{m+1}\right)\right)^k} = \frac{\left(1-\gamma_l\left(1-\alpha_l^{m+1}\right)\right)\gamma_l^h\left(1-\alpha_l^{m+1}\right)^h}{1-\left(\gamma_l\left(1-\alpha_l^{m+1}\right)\right)^{n_r+1}}. \quad (21)$$

We recall that γ_l is the packet loss probability, which we derived in Eq. (9) together with Eqs. (14) and (17), and $1-\alpha_l^{m+1}$ is the probability of successful channel access within $m+1$ backoff stages, where α_l^{m+1} follows from Eq. (5).

The average delay at the h-th attempt is

$$\mathbb{E}[D_{l,h}] = L_s + hL_c + \sum_{l=0}^{h} \mathbb{E}[T_l], \quad (22)$$

where T_l is the backoff stage delay, whereas L_s and L_c are the time periods in number of time units for successful packet transmission and collided packet transmission computed in Eq. (2).

Since the backoff time in each stage k is uniformly distributed in $[0, W_k-1]$, where $W_k = 2^{BE}$, the expected total backoff delay is

$$\mathbb{E}[T_l] = T_{sc} + \sum_{r=0}^{m} \Pr[\mathscr{D}_r|\mathscr{D}]\left(rT_{sc} + \sum_{k=0}^{r}\frac{W_k-1}{2}S_b\right), \quad (23)$$

where T_{sc} is the sensing time in the unslotted mechanism. The event $\mathscr{D}_r$ denotes the occurrence of a busy channel for r consecutive times, and then an idle channel at the $(r+1)$th time. By considering all the possibilities of busy channel during two CCAs, the probability of $\mathscr{D}_r$ is conditioned on the successful sensing event within m attempts $\mathscr{D}$, given that the node senses an idle channel in CCA. It follows that

$$\Pr[\mathscr{D}_r|\mathscr{D}] = \frac{\alpha_l^r}{\sum_{k=0}^{m}\alpha_l^k} = \frac{\alpha_l^r(1-\alpha_l)}{1-\alpha_l^{m+1}}. \quad (24)$$

By applying Eqs. (21)–(24) in Eq. (20), the average delay for successfully received packets is computed. A derivation of the queueing delay is provided in Appendix A. Note that the delay is experienced at the MAC level and is hereby linked to the fading channel through the dependency on α_l and γ_l evaluated in the previous section.

C. Energy Consumption

Here we derive the expression of the energy consumption of the transmitting node of link l as the sum of the contribution in backoff, carrier sense, transmission, reception, idle-queue, and relay states:

$$E_{\mathrm{tot},l} = E_{b,l} + E_{s,l} + E_{t,l} + E_{r,l} + E_{q,l} + E_{x,l}. \qquad (25)$$

In the following, each component of this expression is derived according to the state probabilities in Section III-A. The energy consumption during backoff is

$$\begin{aligned} E_{b,l} &= P_{\mathrm{id}}\tau_l \frac{1}{2}\left(\frac{\sum_{i=0}^{m}\alpha_l^i 2^{m_0+i}}{\sum_{i=0}^{m}\alpha_l^i}+1\right) \\ &= P_{\mathrm{id}}\frac{\tau_l}{2}\left(\frac{\left(1-(2\alpha_l)^{m+1}\right)(1-\alpha_l)}{(1-2\alpha_l)\left(1-\alpha_l^{m+1}\right)}2^{m_0}+1\right), \end{aligned}$$

where P_{id} is the average power consumption in idle-listening state, as we assume that the radio is set in idle-listening state during the backoff stages, The terms in the parentheses represent the average backoff window size with respect to the probability τ_l of having a backoff attempt in any retransmission stage. The energy consumption for carrier sensing is $E_{s,l} = P_{\mathrm{sc}}\tau_l$, where P_{sc} is the average node power consumption in carrier sensing state. The energy consumption during the transmission stage, including ACK reception, is

$$E_{t,l} = (1-\alpha_l)\tau_l\left(P_t L + P_{\mathrm{id}} + \left(P_r(1-\gamma_l) + P_{\mathrm{id}}\gamma_l\right)L_{\mathrm{ack}}\right),$$

where P_{t} and P_{r} are the average node power consumption in transmission and reception respectively, and we assume $t_{\mathrm{m,ack}} = L_{\mathrm{ack}} + 1$ in backoff time units S_b. In the single-hop case, we assume that the node is in sleeping state with negligible energy consumption during inactivity periods without packet generation. Hence, the energy consumption during the idle-queue state is given by $E_{q,l} = P_{\mathrm{s}} b_{\mathrm{idle}}^{(l)}$, where P_{s} is the average node power consumption in sleeping mode, and $b_{\mathrm{idle}}^{(l)}$ is the stationary probability of the idle-queue state (see Appendix B).

In the multi-hop case, relay nodes are in idle-listening state also during the inactivity period (because of the duty cycle policy), and an extra cost for receiving packets and sending ACKs has to be accounted for. This is included in the energy consumption $E_{x,l}$ due to the packets and ACKs of relay nodes based on the routing matrix $\mathbf{M}$,

$$\begin{aligned} E_{x,l} = \sum_{n=1}^{N} M_{n,i}(1-\gamma_n)(1-\alpha_n)\tau_n\left(P_t L + P_{\mathrm{id}}\right. \\ \left. + \left(P_r(1-\gamma_n) + P_{\mathrm{id}}\gamma_n\right)L_{\mathrm{ack}}\right). \end{aligned}$$

where the index i represent the transmitting node of link l.

We validate and show the use of these analytical results in the next section.

V. Performance Evaluations

In this section, we present numerical results for the new model for various settings, network topologies, and operations. We report extensive Monte Carlo simulations to validate the accuracy of the approximations that we have introduced in the model. As discussed in [19], [24], the capture threshold model used in the network simulator ns2 [25] gives unsatisfactory performance when multiple access interference is considered. Therefore, we implemented the IEEE 802.15.4 MAC mechanism in Matlab. The fading channel conditions are reproduced by generating independent random variables in each link and for each generated packet, and the SINR accounts for the cumulative interference power. In the simulations, as well as in the model, we consider that the coherence time of the shadow fading is longer than the packet transmission time, which is in the order of milliseconds, but shorter than the packet generation period, which is in the order of seconds. This is typically true for an IEEE 802.15.4 environment [1]. Moreover, we assume there is one queue with an infinite buffer for each node, which services all links originating from the node. For simplicity, there is no priority between own generated packets and forwarded packets.

The setting of the MAC and physical layer parameters is based on the default specifications of the IEEE 802.15.4 [1]. We perform simulations both for single-hop and multi-hop topologies. As a benchmark, we consider the IEEE 802.15.4 MAC model in [20]. Such a model represent the state of the art for unslotted IEEE 802.15.4 single-hop and multi-hop networks with heterogeneous traffic and hidden terminals.

A. Single-Hop Topologies

In this set of performance results, we consider a single-hop star topology as in Fig. 1(a). We let the number of nodes be $N = 7$, the MAC parameters $m_0 = 3$, $m = 4$, $m_b = 5$, $n_r = 0$, $L = 70$ bytes, $L_{\mathrm{ack}} = 11$ bytes and the physical layer parameters $P_{\mathrm{tx},i} = 0$ dBm, and $k = 2$. We validate our model and study the performance of the network by varying the traffic rate $\lambda_i = \lambda$, $i = 1, \ldots, N$, in the range 0.1–10 pkt/s, the radius $r_{i,0} = r$, $i = 1, \ldots, N$, in the range 0.1–10 m, the spread of the shadow fading $\sigma_i = \sigma$, $i = 1, \ldots, N$, in the range 0–6, and the Nakagami parameter κ in the range 1–3. The IEEE 802.15.4 standard specifies that the carrier sensing threshold is 10 dB above the maximum receiver sensitivity for the physical layer (which is typically around -85 dBm) [1]. Therefore, we show results for different values of the carrier sensing threshold, namely $a = -76$ dBm, $a = -66$ dBm, and $a = -56$ dBm. The outage threshold is not specified by the standard. Experimental measurements for IEEE 802.15.4 show that the minimum SINR that guarantees correct packet reception is about 6 dB [18]. In the following, we show results for different values of the outage threshold, namely, $b = 6$ dB, $b = 10$ dB, and $b = 14$ dB.

In Fig. 2, we report the average reliability over all links by varying the node traffic rate λ. The results are shown for different values of the spread σ and in the absence of multi-path ($f_i = 1$). The model is compared with the results obtained by using the model in [20], which was developed in the absence

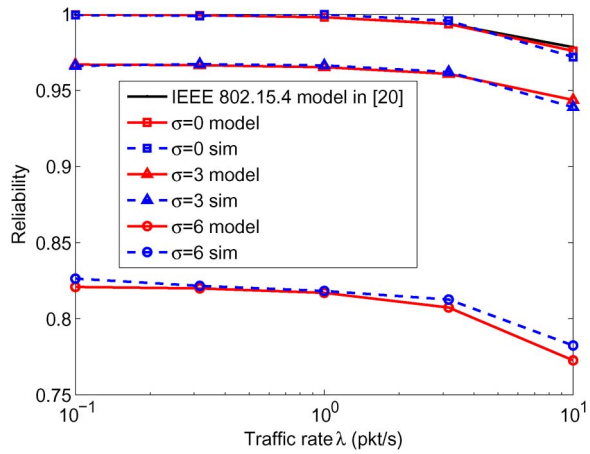

Fig. 2. Reliability versus traffic rate λ for the star network in Fig. 1(a) with $N = 7$ nodes, $r = 1$ m, $a = -76$ dBm, $b = 6$ dB.

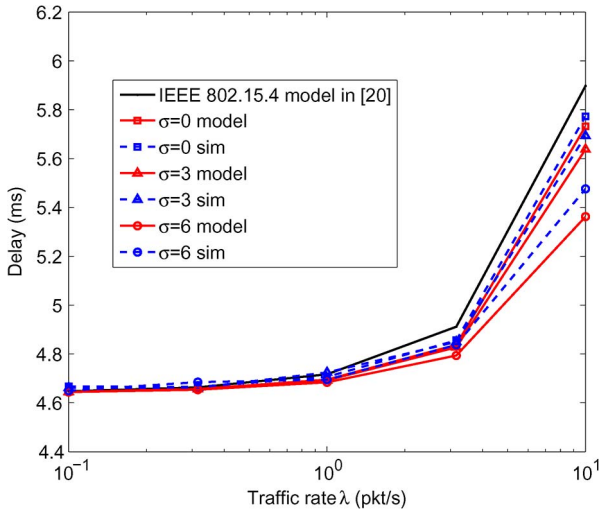

Fig. 3. Delay versus traffic rate λ for the star network in Fig. 1(a) with $N = 7$ nodes, $r = 1$ m, $a = -76$ dBm, $b = 6$ dB.

of a channel model. There is a good matching between the simulations and the analytical expression (19). The reliability decreases as the traffic increases. Indeed, an increase of the traffic generates an increase of the contention level at MAC layer. Our model is close to the ideal case in [20] in the absence of stochastic fluctuation of the channel ($\sigma = 0$). The small gap is due to the presence of thresholds for channel sensing and outage, which reduce the reliability due to possible failures in the CCA mechanism. However, a remarkable aspect is that the impact of shadow fading is more relevant than variations in the traffic. Therefore, a prediction based only on Markov chain analysis of the MAC without including the channel behavior, as typically done in the previous literature, is largely inaccurate to capture the performance of IEEE 802.15.4 wireless networks, especially at larger shadowing spreads.

In Fig. 3, the average delay over all links is reported. Also in this case simulation results follow quite well results obtained from the model as given by Eq. (20). The delay in our model with $\sigma = 0$ is lower than the delay evaluated in the model in [20] due to the effects of thresholds for channel sensing and outage, which reduce the reliability due to possible failures in the CCA mechanism. An increase of traffic leads to an

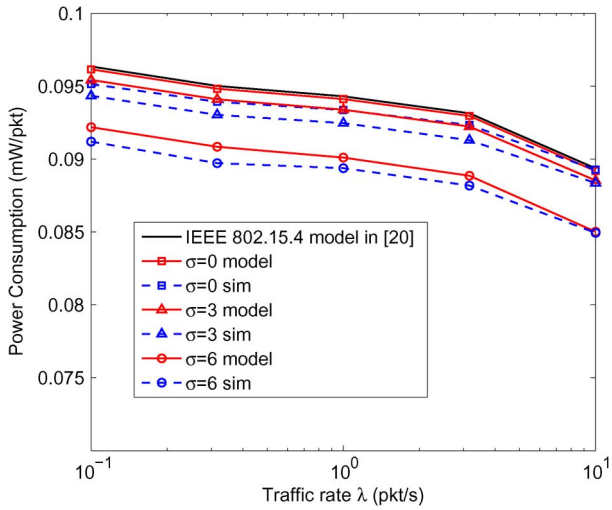

Fig. 4. Power consumption per generated packet versus traffic rate λ for the star network in Fig. 1(a) with $N = 7$ nodes, $r = 1$ m, $a = -76$ dBm, $b = 6$ dB.

increase of the average delay due to the larger number of channel contentions and consequently an increase in the number of backoffs. The spread of shadowing components does not impact on the delay significantly, particularly for low traffic, because lost packets due to fading are not accounted for in the delay computation. When the traffic increases, we note that fading is actually beneficial for the delay. In fact, the delay of successfully received packets reduces by increasing σ. This is because the occurrence of a deep fading reduces the probability of successful transmission. However, since this holds for all nodes, the average number of contending nodes for the CCA may reduce, thus reducing the average delay of successfully received packets. It is not possible to capture this network behavior by using separate models of the IEEE 802.15.4 MAC and physical layers as in the previous literature, since this effect clearly depends on a cross-layer interaction.

In Fig. 4, the average power consumption per generated packet is presented and compared with the analytical expression in Eq. (25). The number of packet transmissions and ACK receptions is the major source of energy expenditure in the network. However, an increase of the traffic leads to a decrease of the power consumption per generated packet due to the smaller number of received ACKs. The power consumption is also reduced when the spread increases. Note that no power control policy is implemented.

In Fig. 5, the average reliability is reported as a function of the radius r for different values of the spread σ. Again, analytical results obtained through Eq. (19) are in good agreement with those provided by simulations. For the ideal channel case (i.e., $\sigma = 0$) the size of the network does not affect the reliability in the range $r = 0.1 - 10$ m. For $\sigma = 6$, the performance degrades significantly as the radius increases. An intermediate behavior is obtained for $\sigma = 3$, where the reliability is comparable to the ideal channel case for short links, but it reduces drastically for $r > 1$ m. The effect is the combination of an increase of the outage probability with the radius (due to the path loss component) and hidden terminals that are not detected by the CCA.

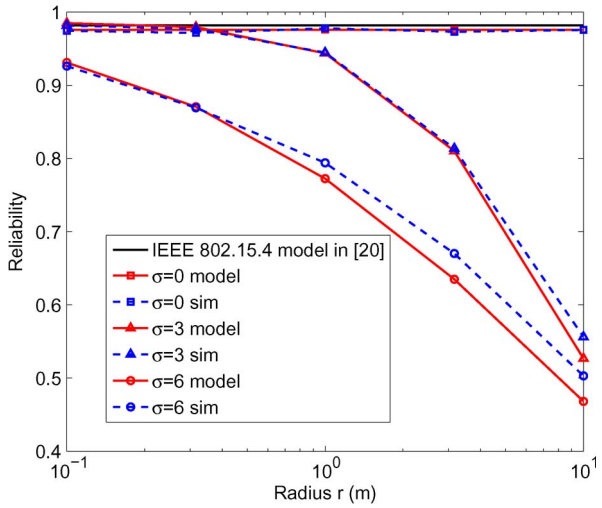

Fig. 5. Reliability versus radius r for the star network in Fig. 1(a) with $N = 7$ nodes, $\lambda = 10$ pkt/s, $a = -76$ dBm, $b = 6$ dB.

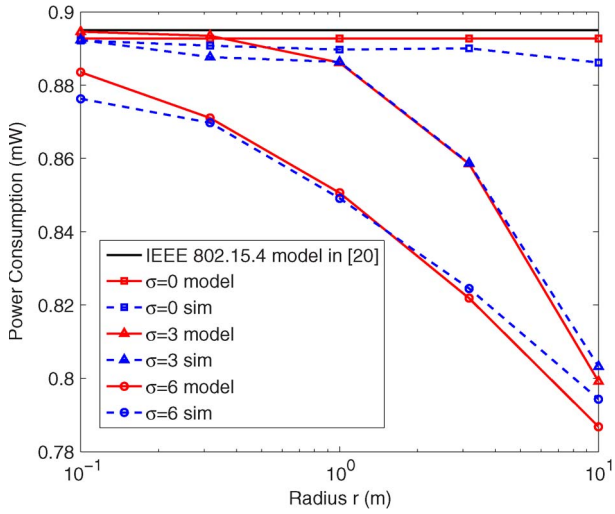

Fig. 7. Power consumption versus radius r for the star network in Fig. 1(a) with $N = 7$ nodes, $\lambda = 10$ pkt/s, $a = -76$ dBm, $b = 6$ dB.

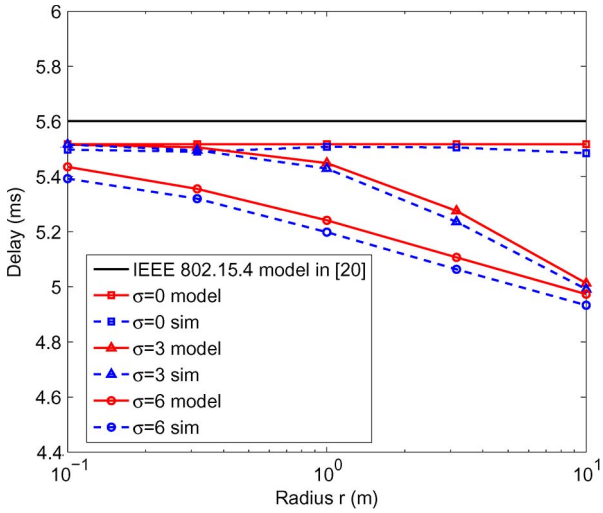

Fig. 6. Delay versus radius r for the star network in Fig. 1(a) with $N = 7$ nodes, $\lambda = 10$ pkt/s, $a = -76$ dBm, $b = 6$ dB.

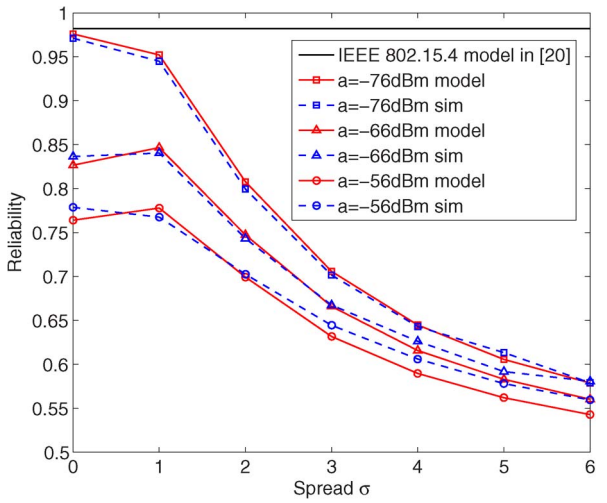

Fig. 8. Reliability versus σ for the star network in Fig. 1(a) with $N = 7$ nodes, $r = 5$ m, $\lambda = 10$ pkt/s, $b = 6$ dB.

In Fig. 6, we report the average delay by varying the radius r for different values of the spread σ. The shadowing affects the delay positively and the effect is more significant for larger inter-node distances: in this case the average number of contending nodes for the free channel assessment reduces, thus the busy channel probability reduces, which in turn decreases the average delay of successfully received packets.

In Fig. 7, the average power consumption by varying r is presented. We notice a similar behavior as for the delay. The power consumption reduces with the fading and the increasing size of the network. Nodes spend less time in the backoff and channel sensing procedure due to reduced number of contending nodes and the number of ACKs.

Fig. 8 shows the average reliability as a function of the shadowing spread σ. The results are plotted for different values of the carrier sensing threshold a. The reliability decreases when the threshold a become larger. The impact of the variation of the threshold a is maximum for $\sigma = 0$, and the gap reduces when the spread σ increases. In Fig. 9, the average delay is plotted as a function of the spread σ. Depending on the threshold a, the delay shows a different behavior when increasing σ: it increases for $a = -76$ dBm and it decreases for $a = -66$ dBm, and $a = -56$ dBm. As we discussed above, the spread σ may reduce the delay under some circumstances. However, when the threshold is large, the average number of contenders is less influenced by the fading and does not decrease significantly, while the busy channel probability becomes dominant and the number of backoffs increases, so that the delay increases as well. Fig. 10 reports the average power consumption by varying the spread σ. The power consumption reduces by increasing the threshold a as a consequence of the smaller number of ACK transmissions, although a maximum consumption is observed for low values of the spread.

In Fig. 11, we plot the average reliability as a function of the spread σ for different values of the outage threshold b. The threshold b does not affect the performance noticeably for $\sigma = 0$, while the gap in the reliability increases with σ. Note that for a high threshold the reliability tends to increase with σ as long

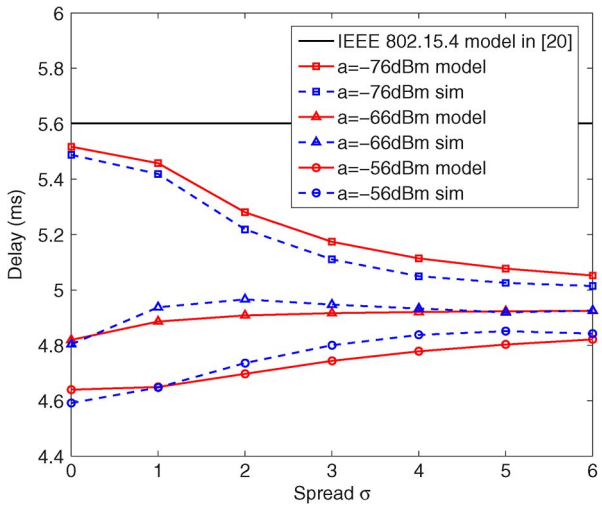

Fig. 9. Delay versus σ for the star network in Fig. 1(a) with $N = 7$ nodes, $r = 5$ m, $\lambda = 10$ pkt/s, $b = 6$ dB.

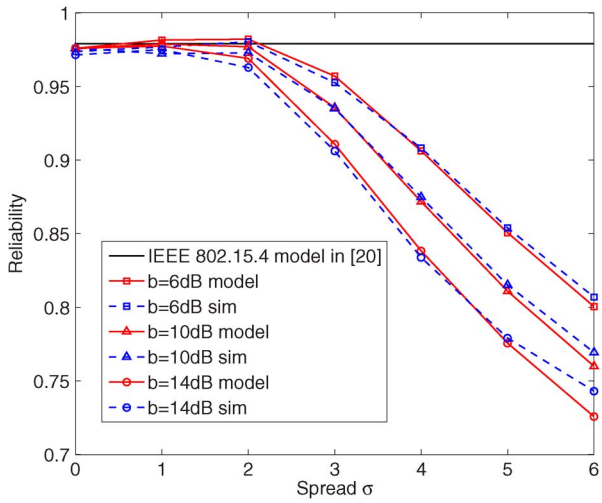

Fig. 11. Reliability versus σ for the star network in Fig. 1(a) with $N = 7$ nodes, $r = 1$ m, $\lambda = 10$ pkt/s, $a = -76$ dB.

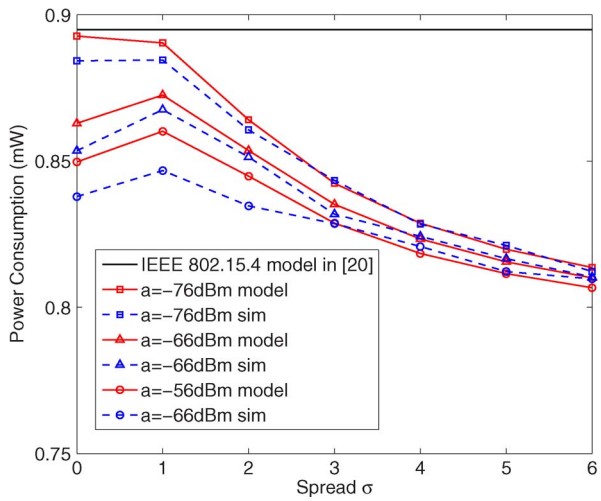

Fig. 10. Power consumption versus σ for the star network in Fig. 1(a) with $N = 7$ nodes, $r = 1$ m, $\lambda = 10$ pkt/s, $b = 6$ dB.

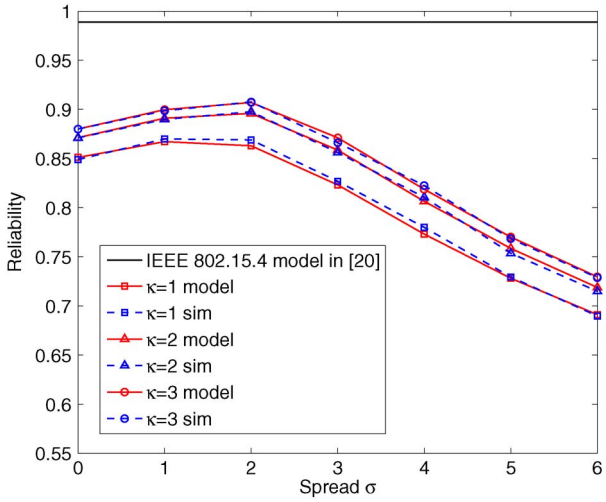

Fig. 12. Reliability versus σ for the star network in Fig. 1(a) with $N = 7$ nodes, $r = 1$ m, $\lambda = 5$ pkt/s, $a = -56$ dB, $b = 6$ dB.

as σ is small or moderate, and it decreases for large spreads. In our setup, a maximum in the reliability is obtained for $\sigma \approx 2$.

In Fig. 12, we report the combined effects of shadow fading and multi-path fading on the reliability. We show the reliability as a function of the spread σ of the shadow fading for different values of the Nakagami parameter κ. We recall that $\kappa = 1$ corresponds to Rayleigh fading. There is a good match between the simulations and the analytical model (19). The effect of the multi-path is a further degradation of the reliability. However, the impact reduces as the Nakagami parameter κ increases and the fading becomes less severe. In fact, for $\kappa \gg 1$, the effect of multi-path becomes negligible. Furthermore, the multi-path fading and the composite channel evidences the presence of the maximum at $\sigma \approx 2$ in the plot of reliability.

B. Multi-Hop Linear Topologies

In this set of performance results, we consider the multi-hop linear topology in Fig. 1(b). The number of nodes is $N = 5$, with the same MAC and physical layer parameters as in the single-hop case. We validate our model and study the performance of the network as a function of the hop distance $r_{i,j}$ in the range $r = 0.1 - 10$ m, and the spread of the shadow fading in the range $\sigma = 0 - 6$. We show results for each hop, and for different values of the carrier sensing threshold $a = -76, 66, 56$ dBm, and outage threshold $b = 6, 10, 14$ dB.

In Fig. 13, the end-to-end reliability is reported from each node to the destination node for different values of the spread σ. The analytical model follows well the simulation results. The end-to-end reliability decreases with the number of hops. This effect is more evident in the presence of shadowing. Fig. 14 shows the end-to-end reliability from the farthest node to the destination by varying the distance r between every two adjacent nodes for different values of the spread σ. The reliability is very sensitive to an increase of the hop distance. In Fig. 15, we show the end-to-end reliability by varying the spread σ of the shadow fading. Results are shown for different values of the carrier sensing threshold a. In Fig. 16, we plot the end-to-end reliability for different values of b. Similar considerations as for the single-hop case applies here. However, for the linear

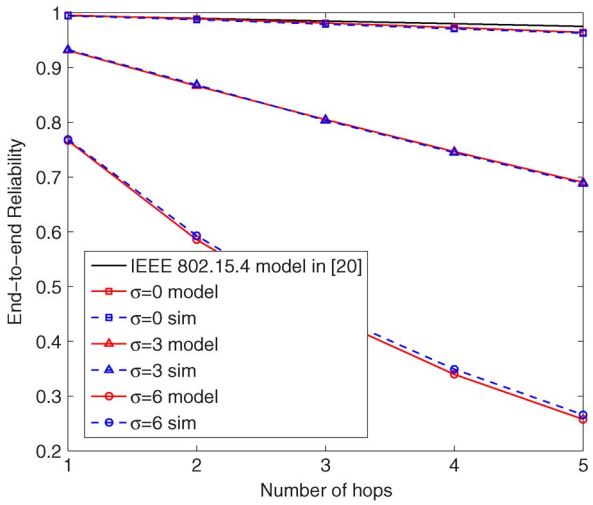

Fig. 13. End-to-end reliability versus number of hops for the linear topology in Fig. 1(b) with $N = 5$ nodes, $r = 1$ m, $\lambda = 2$ pkt/s, $a = -76$ dB, $b = 6$ dB.

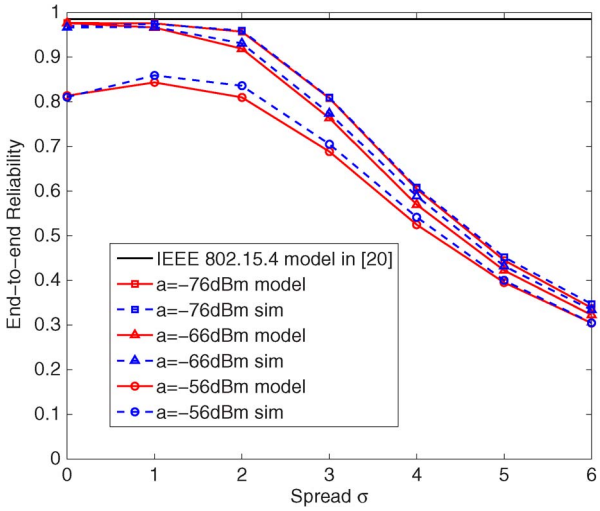

Fig. 15. End-to-end reliability versus σ for the linear topology in Fig. 1(b) with $N = 5$ nodes, $r = 1$ m, $\lambda = 2$ pkt/s, $b = 6$ dB.

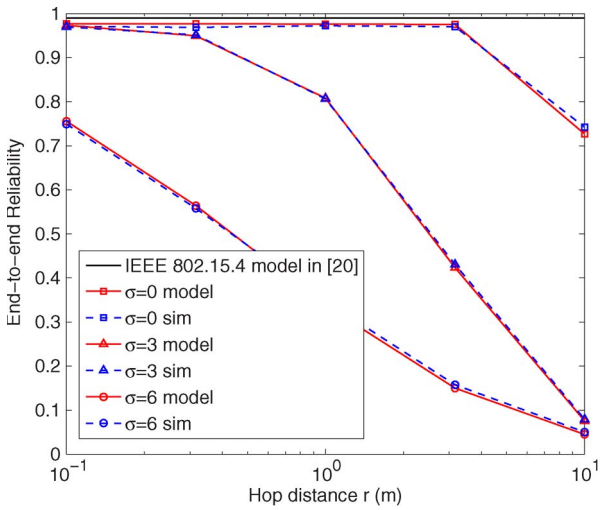

Fig. 14. End-to-end reliability versus hop distance r for the linear topology in Fig. 1(b) with $N = 5$ nodes, $\lambda = 2$ pkt/s, $a = -76$ dB, $b = 6$ dB.

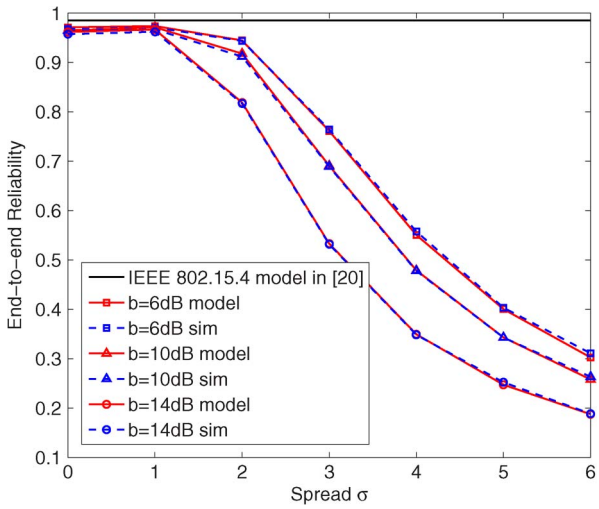

Fig. 16. End-to-end reliability versus σ for the linear topology in Fig. 1(b) with $r = 1$ m, $\lambda = 2$ pkt/s, $a = -76$ dB.

topology, the reduction of the carrier sensing range from $a = -76$ dBm to $a = -66$ dBm influences less the reliability since hidden nodes are often out of range of the receiver, therefore the channel detection failure may not lead to collisions.

C. Multi-Hop Topologies With Multiple End-Devices

We consider the multi-hop topology in Fig. 1(c). We use the same MAC and physical layer parameters as in the single-hop case. We consider the end-to-end reliability as the routing metric and study the performance of the network as a function of the traffic $\lambda_i = \lambda$, $i = 1, \ldots, N$, in the range 0.1–10 pkt/s, the spread of the shadow fading in the range $\sigma = 0 - 6$. Moreover, we show results for different values of the Nakagami parameter $\kappa = 1 - 3$ and threshold $b = 6, 10, 14$ dB.

In Fig. 17, we report the average end-to-end reliability over all the end-devices by varying the node traffic rate. The results are shown for different values of Nakagami parameter κ with the shadowing spread set to $\sigma = 6$. The impact of the Nakagami parameter κ seems more prominent than variation of the traffic. Fig. 18 shows the end-to-end reliability by varying the spread σ for different values of b. Differently to the other topologies, a variation of the outage threshold b has a strong impact on the reliability also for small to moderate shadowing spread. In fact, due to the variable distance between each source-destination pair, the fading and the outage probabilities affect the network noticeably. This effect is well predicted by the developed analytical model.

In Fig. 19, we report the end-to-end reliability for each node for a generic heterogeneous setup of $\lambda = [6\ 4\ 2\ 7\ 5\ 3\ 1]$ pkt/s, and $\sigma = [1\ 3\ 5\ 7\ 2\ 4\ 6]$. The analytical results follow the simulations very closely and the combined effect of different traffic and channel spread for each node is captured accurately.

As a final indication, to provide an idea of the level of traffic saturation with respect to the network capacity, we report that the proposed scenario in Fig. 1(c) with $\lambda = 10$ pkt/s has an offered throughput $S \approx 60$ Kbps, i.e., approximately 60% of the network capacity [1].

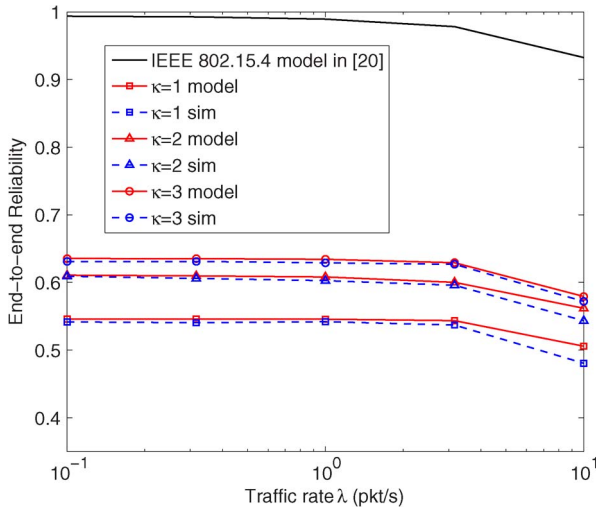

Fig. 17. End-to-end reliability versus traffic rate λ for the multi-hop topology in Fig. 1(c) with $a = -76$ dB, $b = 6$ dB, $\sigma = 6$.

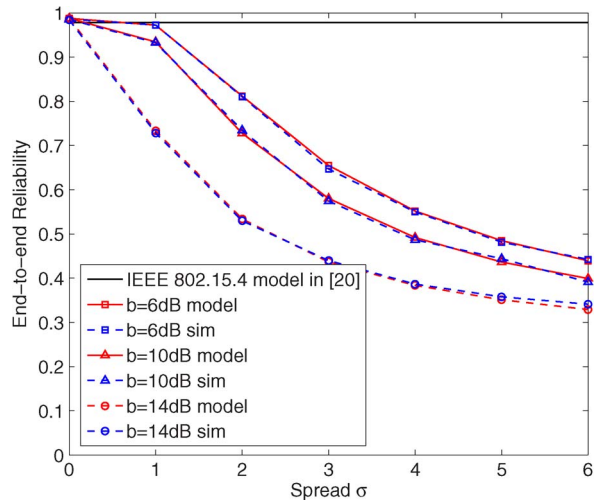

Fig. 18. End-to-end reliability versus σ for the multi-hop topology in Fig. 1(c) with $\lambda = 2$ pkt/s, $a = -76$ dB.

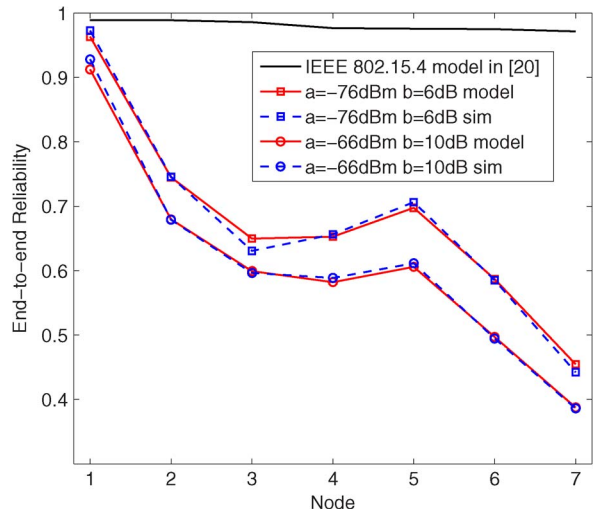

Fig. 19. End-to-end reliability versus node for the multi-hop topology in Fig. 1(c) with $\lambda = [6\ 4\ 2\ 7\ 5\ 3\ 1]$ pkt/s, and $\sigma = [1\ 3\ 5\ 7\ 2\ 4\ 6]$.

VI. Conclusion

In this paper, we proposed an integrated cross-layer model of the MAC and physical layers for unslotted IEEE 802.15.4 networks, by considering explicit effects of multi-path shadow fading channels and the presence of interferers. We studied the impact of fading statistics on the MAC performance in terms of reliability, delay, and power consumption, by varying traffic rates, inter-nodes distances, carrier sensing range, and SINR threshold. We observed that the severity of the fading and the physical layer thresholds have significant and complex effects on all performance indicators, and the effects are well predicted by the new model. In particular, the fading has a relevant negative impact on the reliability. The effect is more evident as traffic and distance between nodes increase. However, depending on the carrier sensing and SINR thresholds, our model shows that a fading with small spread can improve the reliability with respect to the ideal case. The delay for successfully received packets and the power consumption are instead positively affected by the fading and the performance can be optimized by properly tuning the thresholds.

We believe that the design of future WSN-based systems can greatly benefit from the results presented in this paper. As a future work, a tradeoff between reliability, delay, and power consumption can be exploited by proper tuning of routing, MAC, and physical layer parameters. Various routing metrics can be analyzed, and the model extended to multiple sinks.

Appendix A
Queueing Model

We model the packet queue in the buffer as a $M/G/1/K$ queueing system. Denoting as a_k the probability to have k packet arrivals into the buffer of a node during the service time, its probability-generating function (PGF) can be expressed as function of the PGF of the service time $\mathcal{T}_l(z)$ as [26]

$$a_k = \frac{1}{k!}\frac{d^k \mathcal{T}_l(1 - q_l + q_l z)}{dz^k}\bigg|_{z=0}. \tag{26}$$

The steady state probability $p_{l,k}$ that there are k packets in the buffer of the transmitting node in link l after a packet transmission attempt is obtained by solving the following system in a recursive manner [4].

$$\begin{cases} p_{l,k} = p_{l,0}a_k + \sum_{j=1}^{k+1} p_{l,j}a_{k-j+1} & 0 \le k \le B-2, \\ p_{l,B-1} = p_{l,0}\sum_{k=B-1}^{\infty} a_k + \sum_{j=1}^{B-1} p_{l,j}\sum_{k=B-1}^{\infty} a_k. \end{cases} \tag{27}$$

We obtain the probabilities of having a packet to send after a successful transmission $q_{\text{succ},l} = 1 - p_{l,0}$, by inserting the expression of the PGF of the packet service time $\mathcal{T}_l$ into Eq. (26). Similarly, the probability of having a packet to send after channel access failure and retry limits are derived by considering the PGF of the corresponding service time. The PGF of the delay distribution of IEEE 802.15.4 MAC is studied extensively in [27]. Moreover, in case the average queue length is lower than the buffer size B, a good approximation of the empty queue probability can be obtained by using a $M/G/1$ model [28]. For Poisson arrivals with rate λ_i, we obtain

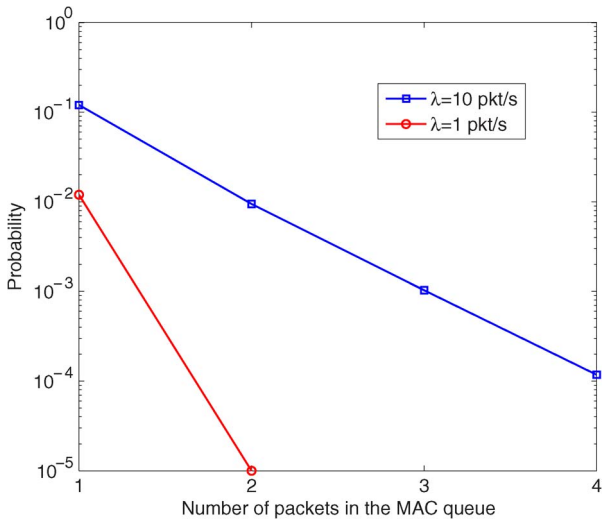

Fig. 20. Probability versus number of packets in the MAC queue, for $\lambda = 1 - 10$ pkt/s, by setting $\sigma = 6$, $a = -76$ dBm, $b = 10$ dB.

$q_{\mathrm{succ},l} = \lambda_i \mathbb{E}\{D_l\}$, where the average service time is computed in Section IV-B. Similar results follow for the probabilities $q_{\mathrm{cf},l}$ and $q_{\mathrm{cr},l}$, by considering the average time for a packet discarded due to channel access failure and due to retry limit, respectively. Note that for multi-hop networks, λ_i considers the total generated and forwarded traffic, according to the analysis in Section III-D. To support our approximation, we study the probability of buffer overflow,

$$p_{\mathrm{overflow},l} = 1 - \sum_{k=0}^{B} p_{l,k} \tag{28}$$

where $p_{l,k}$ is the probability of k packets in the buffer of the transmitting node in link l after a packet transmission attempt in Eq. (27). In Fig. 20, we report the probability of having packets in the MAC queue after a transmission attempt. The simulation results are shown by considering 10^5 generated packets in the topology in Fig. 1(c), by setting traffic $\lambda = 1 - 10$ pkt/s and simulation parameters $\sigma = 6$, $a = -76$ dBm, $b = 10$ dB. The probability of buffer overflow when the buffer size $B > 1$ becomes negligible with respect to the probability of losses due to channel access failure and retry limit. The CC2420 radio transceiver for IEEE 802.15.4 provides separate TX FIFO and RX FIFO buffers of size 256 bytes [29]. Moreover, additional packet queue capacity at MAC layer is provided in sensor mote implementations [30]. Therefore, it is possible to assume that the average queue length at MAC layer is much lower than the buffer capacity.

By using the queueing model described above, the average queueing delay at the source node l can be determined as

$$\mathbb{E}\left[D_l^q\right] = \frac{1}{q_l}\left(\sum_{n=1}^{B-1} n p_{l,k} + B\left(p_{l,0} + q_l \mathbb{E}[D_l] - 1\right)\right) - \mathbb{E}[D_l],$$

where q_l is the total traffic in link l, B is the buffer size, and $p_{l,k}$ is derived in Eq. (27).

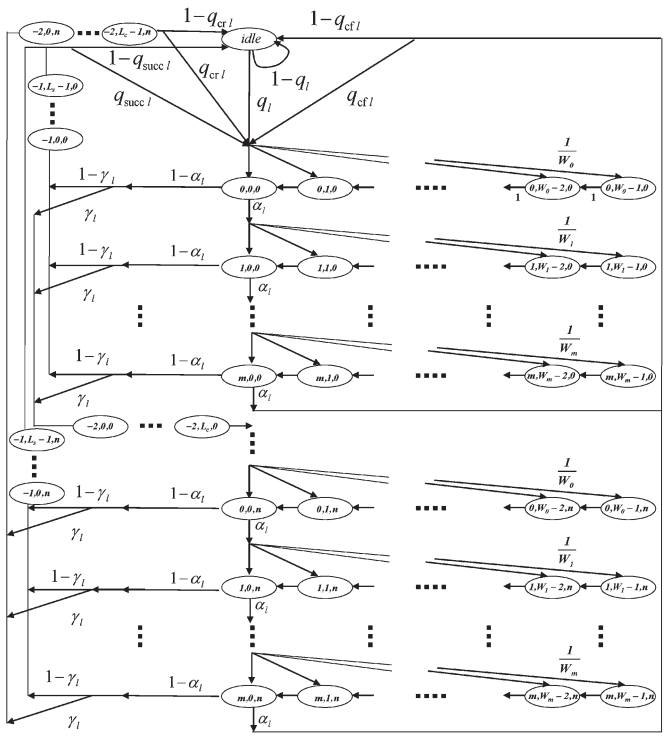

Fig. 21. Markov chain model of the CSMA/CA algorithm of the transmitting node in link l for unslotted IEEE 802.15.4 MAC.

APPENDIX B
MARKOV CHAIN MODEL OF THE IEEE 802.15.4 MAC

Here, we illustrate the Markov chain describing the behavior of the unslotted CSMA/CA mechanism. Let $s_l(t)$, $c_l(t)$ and $r_l(t)$ be the stochastic processes representing the backoff stage, the state of the backoff counter and the state of retransmission counter, respectively, that the transmitting node of link l experiences at time t. Then, the triple $(s_l(t), c_l(t), r_l(t))$ is the three-dimensional per-link Markov chain in Fig. 21, where we use (i, k, j) to denote a particular state.

The Markov chain consists of four main parts corresponding to the idle state, backoff states, CCA states, and packet transmission states. The $idle$ state corresponds to the idle-queue state when the node is waiting for the next packet generation time. The states from $(i, W_m - 1, j)$ to $(i, W_0 - 1, j)$ represent the backoff states. The states $(i, 0, j)$ represent the CCA. The states $(-1, k, j)$ and $(-2, k, j)$ correspond to the successful transmission and packet collision, respectively. The transition probabilities of the chain are

$$\Pr[i,k,j|i,k+1,j] = 1, \qquad \text{for } k \geq 0, \tag{29}$$

$$\Pr[i,k,j|i-1,0,j] = \frac{\alpha_l}{W_i}, \qquad \text{for } i \leq m, \tag{30}$$

$$\Pr[0,k,j|i,0,j-1] = \frac{(1-\alpha_l)\gamma_l}{W_0}, \qquad \text{for } j \leq n_r, \tag{31}$$

$$\Pr[\text{idle}|i,0,j] = (1-q_{\mathrm{succ},l})(1-\gamma_l)\alpha_l, \tag{32}$$

$$\text{for } i < m,\ j < n_r, \tag{33}$$

$$\Pr[\text{idle}|m,0,j] = (1-q_{cf,l})\alpha_l, \qquad \text{for } j < n_r, \tag{34}$$

$$\Pr[\text{idle}|i,0,n_r] = (1-q_{cr,l})(1-\alpha_l), \qquad \text{for } i < m, \tag{35}$$

$$\Pr[\text{idle}|m,0,n_r] = (1-q_{cr,l})(1-\alpha_l) + (1-q_{cf,l})\alpha_l, \quad (36)$$

$$\Pr[0,k,0|\text{idle}] = \frac{q_l}{W_0}, \qquad \text{for } k \le W_0 - 1. \quad (37)$$

We define $b^{(l)}_{i,k,j} = \lim_{t\to\infty} \Pr[s_l(t)=i, c_l(t)=k, r_l(t)=j]$ as the stationary distribution of the Markov chain of Fig. 21.

Owing to the chain regularities and the normalization condition, we know that

$$\sum_{i=0}^{m}\sum_{k=0}^{W_i-1}\sum_{j=0}^{n_r} b^{(l)}_{i,k,j} + \sum_{j=0}^{n_r}\left(\sum_{k=0}^{L_s-1} b^{(l)}_{-1,k,j} + \sum_{k=0}^{L_c-1} b^{(l)}_{-2,k,j}\right) + b^{(l)}_{\text{idle}} = 1. \quad (38)$$

By substituting Eqs. (29)–(37) in Eq. (38), we can derive $b^{(l)}_{0,0,0}$ in Eq. (4) and τ_l by summing up the probabilities of being in the generic sensing stage $b^{(l)}_{i,0,j}$,

$$\tau_l = \sum_{i=0}^{m}\sum_{j=0}^{n_r} b^{(l)}_{i,0,j} = \left(\frac{1-\alpha_l^{m+1}}{1-\alpha_l}\right)\left(\frac{1-\xi_l^{n_r+1}}{1-\xi_l}\right) b^{(l)}_{0,0,0}.$$

APPENDIX C
TABLE OF SYMBOLS

α	busy channel probability during the CCA	r	distance
γ	packet loss probability	t_{ack}	ACK waiting time
κ	Nakagami parameter	t_b	beacon transmission time
λ	traffic generation rate	t_h	backoff delay
ρ	power gain	B	buffer size
σ	spread factor of the shadowing	D	delay
τ	channel access probability	G	number of links
a	detection threshold	L	packet length
b	outage threshold	L_{ack}	ACK length
$b_{i,j,k}$	stationary probability of the Markov chain	$\mathbf{M}$	routing matrix
m	maximum number of backoffs	N	number of nodes
m_0	initial backoff exponent	P_{id}	power consumption in idle-listening state
m_b	max backoff exponent	P_r	power consumption i in reception state
n_r	max number of retransmissions	P_{rx}	received power level
p_{cf}	discarded packet probability due to channel access failure	P_{sc}	power consumption in carrier sensing state
p_{cr}	discarded packet probability due to retransmission failure	P_s	power consumption in sleeping state
$p_{l,k}$	probability of k packets in buffer l	P_t	power consumption in transmission state
p^{det}	detection probability	P_{tx}	transmission power level
p^{fad}	fading probability	P_w	power consumption in wake-up state
p^{out}	outage probability	Q	aggregate traffic (generated and forwarded)
q	packet generation probability in idle state	R	reliability
q_{cf}	packet generation probability after CCA failure	S_b	backoff unit time
q_{cr}	packet generation probability after retry limit	$\mathbf{T}$	traffic distribution matrix
q_{succ}	packet generation probability after successful transmission	W	backoff window

REFERENCES

[1] *IEEE 802.15.4 Wireless Medium Access Control (MAC) and Physical Layer (PHY) Specifications for Low-Rate Wireless Personal Area Networks (WPANs)*, IEEE 802.15.4-2006, 2006. [Online]. Available: http://www.ieee802.org/15/pub/TG4.html

[2] A. Willig, "Recent and emerging topics in wireless industrial communication," *IEEE Trans. Ind. Informat.*, vol. 4, no. 2, pp. 102–124, May 2008.

[3] J. Zheng and M. L. Lee, "Will IEEE 802.15.4 make ubiquitous networking a reality?: A discussion on a potential low power, low bit rate standard," *IEEE Commun. Mag.*, vol. 42, no. 6, pp. 140–146, Jun. 2004.

[4] J. Mišić, S. Shaf, and V. Mišsić, "Performance of a beacon enabled IEEE 802.15.4 cluster with downlink and uplink traffic," *IEEE Trans. Parallel Distrib. Syst.*, vol. 17, no. 4, pp. 361–376, Apr. 2006.

[5] S. Pollin *et al.*, "Performance analysis of slotted carrier sense IEEE 802.15.4 medium access layer," *IEEE Trans. Wireless Commun.*, vol. 7, no. 9, pp. 3359–3371, Sep. 2008.

[6] P. Park, P. Di Marco, P. Soldati, C. Fischione, and K. H. Johansson, "A generalized Markov chain model for effective analysis of slotted IEEE 802.15.4," in *Proc. 6th IEEE Int. Conf. MASS*, 2009, pp. 130–139.

[7] C. Y. Jung, H. Y. Hwang, D. K. Sung, and G. U. Hwang, "Enhanced Markov chain model and throughput analysis of the slotted CSMA/CA for IEEE 802.15.4 under unsaturated traffic conditions," *IEEE Trans. Veh. Technol.*, vol. 58, no. 1, pp. 473–478, Jan. 2009.

[8] J. He, Z. Tang, H.-H. Chen, and Q. Zhang, "An accurate and scalable analytical model for IEEE 802.15.4 slotted CSMA/CA networks," *IEEE Trans. Wireless Commun.*, vol. 8, no. 1, pp. 440–448, Jan. 2009.

[9] C. Buratti, "Performance analysis of IEEE 802.15.4 beacon-enabled mode," *IEEE Trans. Veh. Technol.*, vol. 59, no. 4, pp. 2031–2045, May 2010.

[10] A. Faridi *et al.*, "Comprehensive evaluation of the IEEE 802.15.4 MAC layer performance with retransmissions," *IEEE Trans. Veh. Technol.*, vol. 59, no. 8, pp. 3917–3932, Oct. 2010.

[11] G. Bianchi, "Performance analysis of the IEEE 802.11 distributed coordination function," *IEEE J. Sel. Areas Commun.*, vol. 18, no. 3, pp. 535–547, Mar. 2000.

[12] M.-H. Zayani, V. Gauthier, and D. Zeghlache, "A joint model for IEEE 802.15.4 physical and medium access control layers," in *Proc. 7th IWCMC*, 2011, pp. 814–819.

[13] X. Yang and N. Vaidya, "On physical carrier sensing in wireless ad hoc networks," in *Proc. 24th IEEE INFOCOM*, 2005, pp. 2525–2535.

[14] F. Daneshgaran, M. Laddomada, F. Mesiti, and M. Mondin, "Unsaturated throughput analysis of IEEE 802.11 in presence of non ideal transmission channel and capture effects," *IEEE Trans. Wireless Commun.*, vol. 7, no. 4, pp. 1276–1286, Apr. 2008.

[15] D. Hoang and R. Iltis, "Performance evaluation of multi-hop CSMA/CA networks in fading environments," *IEEE Trans. Commun.*, vol. 56, no. 1, pp. 112–125, Jan. 2008.

[16] E. J. Leonardo and M. D. Yacoub, "Exact formulations for the throughput of IEEE 802.11 DCF in Hoyt, Rice, Nakagami-m fading channels," *IEEE Trans. Wireless Commun.*, vol. 12, no. 5, pp. 2261–2271, May 2013.

[17] G. Sutton, R. Liu, and I. Collings, "Modelling IEEE 802.11 DCF heterogeneous networks with Rayleigh fading and capture," *IEEE Trans. Commun.*, vol. 61, no. 8, pp. 3336–3348, Aug. 2013.

[18] C. Gezer, C. Buratti, and R. Verdone, "Capture effect in IEEE 802.15.4 networks: Modelling and experimentation," in *Proc. 5th IEEE ISWPC*, 2010, pp. 204–209.

[19] A. Iyer, C. Rosenberg, and A. Karnik, "What is the right model for wireless channel interference?" *IEEE Trans. Wireless Commun.*, vol. 8, no. 5, pp. 2662–2671, May 2009.

[20] P. Di Marco, P. Park, C. Fischione, and K. H. Johansson, "Analytical modeling of multi-hop IEEE 802.15.4 networks," *IEEE Trans. Veh. Technol.*, vol. 61, no. 7, pp. 3191–3208, Sep. 2012.

[21] M. Pratesi, F. Santucci, and F. Graziosi, "Generalized moment matching for the linear combination of lognormal RVS: Application to outage analysis in wireless systems," *IEEE Trans. Wireless Commun.*, vol. 5, no. 5, pp. 1122–1132, May 2006.

[22] C. Fischione, F. Graziosi, and F. Santucci, "Approximation for a sum of on-off log-normal processes with wireless applications," *IEEE Trans. Commun.*, vol. 55, no. 9, pp. 1822–1822, Sep. 2007.

[23] D. P. Bertsekas and J. N. Tsitsiklis, *Parallel and Distributed Computation: Numerical Methods*. Belmont, MA, USA: Athena Scientific, 1997.

[24] M. Al-Bado, C. Sengul, and R. Merz, "What details are needed for wireless simulations?—A study of a site-specific indoor wireless model," in *Proc. 31st INFOCOM*, 2012, pp. 289–297.

[25] The ns2 Network Simulator 2011. [Online]. Available: http://www.isi.edu/nsnam/ns/

[26] H. Takagi, *Queueing Analysis: Volume 2 Finite Systems*. Amsterdam, The Netherlands: North Holland, 1993.

[27] P. Park, P. Di Marco, C. Fischione, and K. H. Johansson, "Delay distribution analysis of wireless personal area networks," in *Proc. IEEE CDC*, 2012, pp. 5864–5869.

[28] D. Malone, K. Duffy, and D. Leith, "Modeling the 802.11 distributed coordination function in nonsaturated heterogeneous conditions," *IEEE/ACM Trans. Netw.*, vol. 15, no. 1, pp. 159–172, Feb. 2007.

[29] *CC2420 Data Sheet*, Chipcon, Oslo, Norway, 2005. [Online]. Available: http://www.ti.com/product/CC2420/technicaldocuments

[30] The TinyOS Community Forum 2010. [Online]. Available: http://www.tinyos.net

Piergiuseppe Di Marco (M'13) received the M.Sc. degree in telecommunications engineering from the University of L'Aquila, Italy, in 2008 and the Ph.D. degree in telecommunications at the Royal Institute of Technology, Sweden, in 2013. He is a post-doctoral researcher at the Center of Excellence DEWS, University of L'Aquila and the ACCESS Linnaeus Centre, School of Electrical Engineering, Royal Institute of Technology, Sweden. Dr. Di Marco was a visiting scholar at UC Berkeley in 2011, and a visiting researcher in Ericsson in 2014. His research interests include modeling, design, and optimization in wireless networks, multiple access protocols, routing, and networked control applications. He received best paper awards at the IEEE MASS 2009 and from the IEEE Sweden VT-COM-IT Chapter in 2013.

Carlo Fischione (M'06) received the Ph.D. degree in electrical and information engineering in 2005, and the Dr.Eng. degree in electronic engineering in 2001 from University of L'Aquila, L'Aquila, Italy. He is a tenured Associate Professor at the Royal Institute of Technology (KTH), Electrical Engineering and ACCESS Linnaeus Center, Sweden. He held research positions at UC Berkeley and Royal Institute of Technology. His research interests include optimization and parallel computation with applications to wireless sensor networks, networked control systems, and wireless networks. He received numerous awards, including the best paper award from the IEEE Transactions on Industrial Informatics of 2007, the best paper awards at IEEE MASS 2005 and IEEE MASS 2009, the Best Business Idea award from VentureCup East Sweden, 2010, the Ferdinando Filauro award from University of L'Aquila, Italy, 2003, the Higher Education award from Abruzzo Region Government, Italy, 2004, and the Junior Research award from Swedish Research Council, 2007, the Silver Ear of Wheat award in history from the Municipality of Tornimparte, Italy, 2012. He has chaired or served as a TPC member of several international conferences and is serving as referee for technical journals. He is member of SIAM.

Fortunato Santucci (SM'00) was born in L'Aquila, Italy, in 1964. He received the laurea degree and the Ph.D. degree in electronic engineering from the University of L'Aquila, L'Aquila, Italy, in 1989 and 1994, respectively. In 1989 he was with Selenia Spazio, Rome. In 1991–1992 he was at the Solid State Electronics Institute (IESS) of the National Research Council (CNR), Rome. Since 1994 he has been with the University of L'Aquila, where he currently holds the position of Associate Professor in the Dept. of Information Engineering, Computer Science and Mathematics, and is Chair of the Telecommunications Engineering program. He was a visiting researcher at the University of Victoria, BC. His current research activity is focused on communication theory, access control and radio resource management in mobile radio systems, technologies and architectures for wireless embedded networks. He has served as an Editor for the IEEE TRANSACTIONS ON COMMUNICATIONS from 2000 to 2013, for Kluwer Telecommunications Systems and Hindawi. He is in the IEEE Communications Theory Committee. He is vice-director of the Center of Excellence DEWS at the University of L'Aquila, in the board of the Radiolabs consortium, and in the General Assembly of CNIT. He is a co-founder of WEST Aquila srl, a spin-off of the University of L'Aquila.

Karl Henrik Johansson (F'13) received the M.Sc. and the Ph.D. degrees in electrical engineering from Lund University, Sweden. He is Director of the ACCESS Linnaeus Centre and Professor at the School of Electrical Engineering, KTH Royal Institute of Technology, Sweden. He is a Wallenberg Scholar and has held a six-year Senior Researcher Position with the Swedish Research Council. He is also heading the Stockholm Strategic Research Area ICT The Next Generation. He has held visiting positions at UC Berkeley (1998–2000) and California Institute of Technology (2006–2007). His research interests are in networked control systems, hybrid and embedded system, and applications in transportation, energy, and automation systems. He has been a member of the IEEE Control Systems Society Board of Governors and the Chair of the IFAC Technical Committee on Networked Systems. He has been on the Editorial Boards of several journals, including Automatica, IEEE TRANSACTIONS ON AUTOMATIC CONTROL, and IET Control Theory and Applications. He is currently on the Editorial Board of IEEE TRANSACTIONS ON CONTROL OF NETWORK SYSTEMS and the European Journal of Control. He has been Guest Editor for special issues of the IEEE TRANSACTIONS ON AUTOMATIC CONTROL. He was the General Chair of the ACM/IEEE CPS Week 2010 in Stockholm and IPC Chair of many conferences. He has served on the Executive Committees of several European research projects. He received the Best Paper Award at IEEE MASS 2009 and the Best Theory Paper Award of the World Congress on Intelligent Control and Automation in 2014. In 2009 he was awarded Wallenberg Scholar by the Knut and Alice Wallenberg Foundation. He was awarded an Individual Grant for the Advancement of Research Leaders from the Swedish Foundation for Strategic Research in 2005. He received the triennial Young Author Prize from IFAC in 1996 and the Peccei Award from the International Institute of System Analysis, Austria, in 1993. He received Young Researcher Awards from Scania in 1996 and from Ericsson in 1998 and 1999.